© Strojniški vestnik (43) št. 11-12, str. 483-496, 1997
Tiskano v Sloveniji. Vse pravice pridržane.
UDK 629.1.072.5:519.6
Izvirni znanstveni članek

© Journal of Mechanical Engineering (43) No. 11-12, pp. 483-496, 1997
Printed in Slovenia. All rights reserved.
UDC 629.1.072.5:519.6
Original scientific paper

SV:0039-2480(97)6-R2

Numerična obravnava aerodinamike vozil
Numerical Analysis of Vehicle Aerodynamics

ZORAN ŽUNIČ - LEOPOLD ŠKERGET

Primerjali smo tri različne turbulentne modele k-ε z dušilnimi funkcijami: Lam-Bremhorstovega, Naganovega in Fan-Lakshminarayana-Barnettovega. Reynoldsove enačbe za časovno povprečene spremenljivke toka tekočine smo reševali z metodo končnih prostornin višjega reda. Modele smo testirali na primeru toka v kanalu s stopnico in rezultate primerjali z meritvami Rucka in Makiole. Izbrali smo najboljši model in z njim izračunali tokovno polje okoli avtobusa ter koeficient zračnega upora.

Ključne besede: aerodinamika vozil, analize numerične, tok v kanalu, tok turbulentni, metode končnih volumnov

In this paper a comparison is made between three different k-ε low-Reynolds turbulence models. Lam-Bremhorst's, Nagano's and Fan-Lakshminarayana-Barnett's models were used. Reynolds equations for time averaged fluid flow variables are solved by the higher order finite volume method. All models have been tested against a range of measurements by Ruck and Makiola for backward facing step flow. The best model was chosen and the flow field around bus and drag coefficient were calculated.

Keywords: vehicle aerodynamic, numerical analysis, flow in channel, turbulent flow, finite volume methods

1 VODILNE ENAČBE

Našo pozornost bomo omejili na nestisljiv tok. Povprečene Reynoldsove enačbe ohranitve mase in gibalne količine, zapisane v konzervativni obliki, so:

1 GOVERNING EQUATIONS

Let us confine our attention to incompressible flow. The Reynolds averaged equations of motion (continuity and momentum) in conservation form are:

$$\frac{\partial \overline{u}_i}{\partial x_i} = 0 \qquad (1),$$

$$\rho\frac{\partial \overline{u}_i}{\partial t} + \rho\frac{\partial}{\partial x_j}(\overline{u}_j\overline{u}_i) = -\frac{\partial \overline{p}}{\partial x_i} + \frac{\partial}{\partial x_j}\left((\mu+\mu_T)(\frac{\partial \overline{u}_i}{\partial x_j} + \frac{\partial \overline{u}_j}{\partial x_i})\right) \qquad (2).$$

Turbulentno viskoznost μ_T računamo z:

Turbulent viscosity μ_T is calculated as:

$$\mu_T = \rho C_\mu f_\mu \frac{k^2}{\varepsilon} \qquad (3).$$

V enačbi turbulentne viskoznosti se pojavljata spremenljivki k, turbulentna kinetična energija in ε, turbulentni raztros. Za vsako zapišemo ločeno prenosni enačbi za turbulentno kinetično energijo:

There are two variables in the equation for turbulent viscosity, k being turbulent kinetic energy and ε turbulent dissipation. We write the different transport equations for turbulent kinetic energy as:

$$\rho\frac{\partial k}{\partial t} + \rho\overline{u}_j\frac{\partial k}{\partial x_j} = P - \rho\varepsilon - \rho D + \frac{\partial}{\partial x_j}\left((\mu + \frac{\mu_T}{\sigma_k})\frac{\partial k}{\partial x_j}\right) \qquad (4)$$

ter za turbulentni raztros:

and for turbulent dissipation:

$$\rho\frac{\partial \varepsilon}{\partial t} + \rho\overline{u}_j\frac{\partial \varepsilon}{\partial x_j} = C_{\varepsilon 1} f_1 \frac{\varepsilon}{k}P - C_{\varepsilon 2} f_2 \rho\frac{\varepsilon^2}{k} + \rho E + \frac{\partial}{\partial x_j}\left((\mu + \frac{\mu_T}{\sigma_\varepsilon})\frac{\partial \varepsilon}{\partial x_j}\right) \qquad (5).$$

Izvorni člen P definiramo z:

The production term P is defined as:

$$P = \mu_T\left(\frac{\partial \overline{u}_i}{\partial x_j} + \frac{\partial \overline{u}_j}{\partial x_i}\right)\frac{\partial \overline{u}_i}{\partial x_j} \qquad (6).$$

Enačbe (3) do (5) vsebujejo pet dušilnih funkcij: f_μ, f_1, f_2, D in E, ki so odvisne od enega ali več turbulentnih Reynoldsovih števil:

Equations (3) to (5) contain five empirical damping functions, f_μ, f_1, f_2, D and E, which depend upon one or more of following turbulent Reynolds numbers:

$$Re_T = \frac{k^2}{\nu\varepsilon}, \quad R_y = \frac{y\sqrt{k}}{\nu}, \quad Re_\tau = \frac{y\,u_\tau}{\nu} \qquad (7).$$

Od pravilne izbire dušilnih funkcij je v veliki meri odvisna natančnost izračuna. Tako je z leti veliko število raziskovalcev razvilo svoje turbulentne modele, ki se med seboj razlikujejo le po izbiri dušilnih funkcij in posameznih konstant.

The right choice of dumping functions is of main importance for the accuracy of computation. In the past, many researchers developed their own turbulence models and the only difference between models is the choice of dumping functions and model constants.

2 TURBULENTNI MODELI k-ε Z DUŠILNIMI FUNKCIJAMI

2 TURBULENT k-ε MODELS WITH DUMPING FUNCTIONS

V naših izračunih smo uporabljali tri različne turbulentne modele: Lam-Bremhorstov [3], Naganov [4] in Fan-Lakshminarayana-Barnettov model [1]. Dušilne funkcije in konstante posameznih modelov so podane v preglednici 1.

We used three different turbulence models for calculation, , Lam-Bremhorst's [3], Nagano's [4] in Fan-Lakshminarayana-Barnett's model [1]. Dumping functions and model constants are given in Table 1.

Preglednica 1. *Dušilne funkcije in konstante turbulentnih modelov*
Table 1. *Dumping functions and turbulent model constants*

Model		C_μ	$C_{\varepsilon1}$	$C_{\varepsilon2}$	σ_k	σ_ε	ε_w
Lam-Bremhorst	LB	0,09	1,44	1,92	1,0	1,3	$\frac{\partial\varepsilon}{\partial y}=0$
Nagano	NAG	0,09	1,45	1,9	1,0	1,3	$\varepsilon=0$
Fan-Lakshminarayana-Barnett	FLB	0,09	1,39	1,8	1,0	1,3	$\frac{\partial\varepsilon}{\partial y}=0$

LB	$f_\mu = (1-e^{-0,0165R_y})^2(1+\frac{20,5}{Re_T})$ $f_1 = 1+(\frac{0,05}{f_\mu})^3$ $f_2 = 1-e^{-Re_T^2}$ $D=0$ $E=0$
NAG	$f_\mu = \left(1-\exp(-\frac{Re_\tau}{26,5})\right)^2$ $f_1=1$ $f_2 = 1-0,3\exp(-Re_T^2)$ $D = 2\nu(\frac{\partial\sqrt{k}}{\partial x_j})^2$ $E = \nu\nu_T(1-f_\mu)(\frac{\partial^2\bar{u}_i}{\partial x_j\partial x_k})^2$
FLB	$f_\mu = 0,4\frac{f_w}{\sqrt{Re_T}} + (1-0,4\frac{f_w}{\sqrt{Re_T}})(1-e^{-R_y/42,63})^3$ $f_1=1$ $f_2 = (1-e^{-(Re_T/6)^2})f_w^2$ $f_w = 1-exp\Big(-\frac{\sqrt{R_y}}{2,30}+(\frac{\sqrt{R_y}}{2,30}-\frac{R_y}{8,89})(1-e^{-R_y/20})^3\Big)$ $D=0$ $E=0$

3 REŠEVANJE REYNOLDSOVIH ENAČB

Sistem povprečenih Reynoldsovih enačb ravninskega toka nestisljive tekočine ob upoštevanju umetne stisljivosti skupaj s prenosnima enačbama turbulentne kinetične energije ter turbulentnega raztrosa v lokalnem koordinatnem sistemu $\xi = \xi(x,z)$ ter $\zeta = \zeta(x,z)$ ob uporabi brezdimenzijskih spremenljivk zapišemo v konzervativni obliki kot eno samo vektorsko enačbo:

3 SOLVING OF REYNOLDS EQUATIONS

The Reynolds averaged equations - with the artificial compressibility term added, and with transport equations for turbulent kinetic energy and turbulent dissipation - can be expressed in generalized coordinates $\xi = \xi(x,z)$, $\zeta = \zeta(x,z)$ and dimensionless form as a one vector equation:

$$\frac{\partial \mathcal{Q}}{\partial t} + \frac{\partial \mathcal{E}}{\partial \xi} + \frac{\partial \mathcal{G}}{\partial \zeta} = \frac{\partial \mathcal{E}_{vis}}{\partial \xi} + \frac{\partial \mathcal{G}_{vis}}{\partial \zeta} + \mathcal{S}, \tag{8}$$

kjer so: / where:

$$\mathcal{Q} = JQ \tag{9a}$$

$$\mathcal{E} = J\left(\frac{\partial \xi}{\partial x}E + \frac{\partial \xi}{\partial z}G\right) \tag{9b}$$

$$\mathcal{G} = J\left(\frac{\partial \zeta}{\partial x}E + \frac{\partial \zeta}{\partial z}G\right) \tag{9c}$$

$$\mathcal{E}_{vis} = J\left(\frac{\partial \xi}{\partial x}E_{vis} + \frac{\partial \xi}{\partial z}G_{vis}\right) \tag{9d}$$

$$\mathcal{G}_{vis} = J\left(\frac{\partial \zeta}{\partial x}E_{vis} + \frac{\partial \zeta}{\partial z}G_{vis}\right) \tag{9e}$$

$$\mathcal{S} = JS \tag{9f}$$

in / and

$$Q = \left\{\, p/\beta,\ u,\ w,\ k,\ \varepsilon \,\right\} \tag{10a}$$

$$E = \left\{\, u,\ u^2 + p,\ uw,\ uk,\ u\varepsilon \,\right\}, \qquad G = \left\{\, w,\ uw,\ w^2 + p,\ wk,\ w\varepsilon \,\right\} \tag{10b}$$

$$E_{vis} = \left\{\, 0,\ \tilde{\tau}_{xx},\ \tilde{\tau}_{xz},\ \tilde{k}_x,\ \tilde{\varepsilon}_x \,\right\}, \qquad G_{vis} = \left\{\, 0,\ \tilde{\tau}_{xz},\ \tilde{\tau}_{zz},\ \tilde{k}_z,\ \tilde{\varepsilon}_z \,\right\} \tag{10c}$$

$$S = \left\{\, 0,\ 0,\ 0,\ P - \epsilon,\ C_{\epsilon 1} f_1 \frac{\epsilon}{k} P - C_{\epsilon 2} f_2 \frac{\epsilon^2}{k} \,\right\} \tag{10d}$$

$$\tilde{\tau} = (\mu + \mu_T)\begin{bmatrix} 2\dfrac{\partial u}{\partial x} & \dfrac{\partial u}{\partial z} + \dfrac{\partial w}{\partial x} \\[2ex] \dfrac{\partial u}{\partial z} + \dfrac{\partial w}{\partial x} & 2\dfrac{\partial w}{\partial z} \end{bmatrix} \tag{10e}$$

$$\tilde{k} = (\mu + \frac{\mu_T}{\sigma_k})\left\{\, \frac{\partial k}{\partial x},\ \frac{\partial k}{\partial z} \,\right\} \tag{10f}$$

$$\tilde{\varepsilon} = (\mu + \frac{\mu_T}{\sigma_\varepsilon})\left\{\, \frac{\partial \varepsilon}{\partial x},\ \frac{\partial \varepsilon}{\partial z} \,\right\} \tag{10g}$$

$$J = \frac{\partial x}{\partial \xi}\frac{\partial z}{\partial \zeta} - \frac{\partial x}{\partial \zeta}\frac{\partial z}{\partial \xi} \tag{10h}$$

Enačbo (8) rešujemo z metodo končnih prostornin. Za aproksimacijo konvektivnih tokov smo uporabili metodo karakteristik. Po tej metodi računamo konvektivne tokove s tokovi na karakteristiki, glede na predznak lokalne lastne vrednosti Riemannovega sistema. Za aproksimacijo difuzijskih tokov smo uporabili "zgornje" končne razlike za mešane odvode in osrednje končne razlike za odvode drugega reda. Izvorne člene smo aproksimirali z osrednjimi končnimi razlikami. Integracijo po času smo izvedli z metodo Runge-Kutta četrtega reda. Opisani postopek je povzet po Drikakisu [2].

Equation (8) is solved using the finite volume method. The characteristics based method (CBM) is used for the discretization of the convective fluxes. The CBM is based on a characteristic flux averaging of the inviscid fluxes according to the sign of the local eigenvalue of the Riemann's system. For discretization of the viscous fluxes an 'upwind'-type scheme for the cross derivatives and central discretization for the second-order derivatives were used. For the time integration the explicit fourth-order Runge-Kutta time stepping method was employed. This method was developed by Drikakis [2].

4 RAČUNSKI PRIMERI

4 EXAMPLES

4. 1 Turbulentni tok skozi kanal s stopnico

Uporabljene modele smo testirali na primeru turbulentnega toka v kanalu s stopnico. Za ta primer smo se odločili, ker je dovolj zahteven, da se pokažejo pomanjkljivosti posameznih modelov, obenem pa imamo dovolj eksperimentalnih rezultatov, s katerimi lahko primerjamo natančnost naših izračunov. Računali smo tok za vrednost Reynoldsovega števila $Re = 15000$, ki smo ga definirali po višini kanala na vstopu in z največjo hitrostjo toka. Slika 1 prikazuje obliko problema.

4. 1 Turbulent flow in channel with a step

The different models described here have been tested on the case of the channel flow with a backwards facing step. This case is complex enough to show the drawbacks of the model and at the same time there are many experiments to compare with the calculated results. The flow was calculated for Reynolds number Re=15000. The Reynolds number was based on channel inlet height and maximum inlet velocity. The shape of the problem is shown in Figure 1.

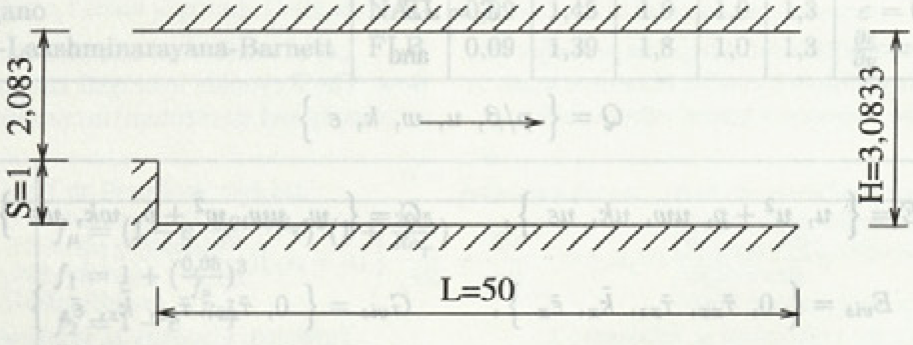

Sl. 1. *Kanal s stopnico: oblika in robne razmere*
Fig. 1. *Backwards facing step: shape and boundary conditions*

Robne razmere so bile naslednje:
- vstop: $\partial p/\partial n = 0$, u = izmerjen, $w = 0$, $k = 0{,}01$, $\varepsilon = C_\mu \cdot k^{3/2}/0{,}02$,
- izstop: $p = 0$, $\partial u/\partial n = 0$, $\partial w/\partial n = 0$, $\partial k/\partial n = 0$, $\partial \varepsilon/\partial n = 0$,
- stene: $\partial p/\partial n = 0$, $u = 0$, $w = 0$, $k = 0$, ε odvisen od modela

Boundary conditions:
- inlet: $\partial p/\partial n = 0$, u = measured, $w = 0$, $k = 0.01$, $\varepsilon = C_\mu \cdot k^{3/2}/0.02$,
- outlet: $p = 0$, $\partial u/\partial n = 0$, $\partial w/\partial n = 0$, $\partial k/\partial n = 0$, $\partial \varepsilon/\partial n = 0$,
- wall: $\partial p/\partial n = 0$, $u = 0$, $w = 0$, $k = 0$, ε depends on model

Uporabili smo tri različne gostote mrež: 30 × 20, 50 × 30 in 80 × 50.

Three different mesh sizes were used: 30 × 20, 50 × 30 and 80 × 50.

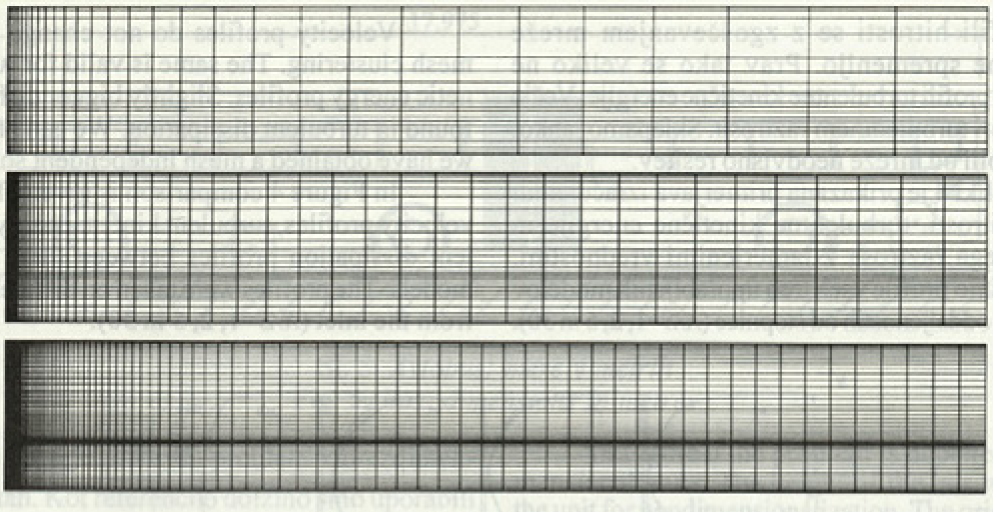

Sl. 2. *Diskretizacija območja*
Fig. 2. *Domain discretization*

Rezultate smo primerjali z meritvami Rucka in Makiole [5]. Zanimala nas je konvergenca rešitve z zgoščevanjem mreže ter natančnost posameznih modelov.

Na sliki 3 je prikazana primerjava izračunanih profilov hitrosti, turbulentne kinetične energije in turbulentnega raztrosa za posamezne gostote mrež na različnih oddaljenostih od stopnice (X/S = 1, 2, 5 in 30). Uporabili smo rezultate Fan-Lakshminarayana-Barnettovega modela.

The results were compared against measurements by Ruck and Makiola [5]. We investigated the convergence of the solution with increasing of mesh size and accuracy of turbulence models.

In Figure 3 comparison is given of the calculated velocity profiles, turbulent kinetic energy and turbulent dissipation profiles between three different meshes. The profiles were taken on different distances from the inlet (X/S=1, 2, 5 and 30). We compared the results of the Fan-Lakshminarayana-Barnett model.

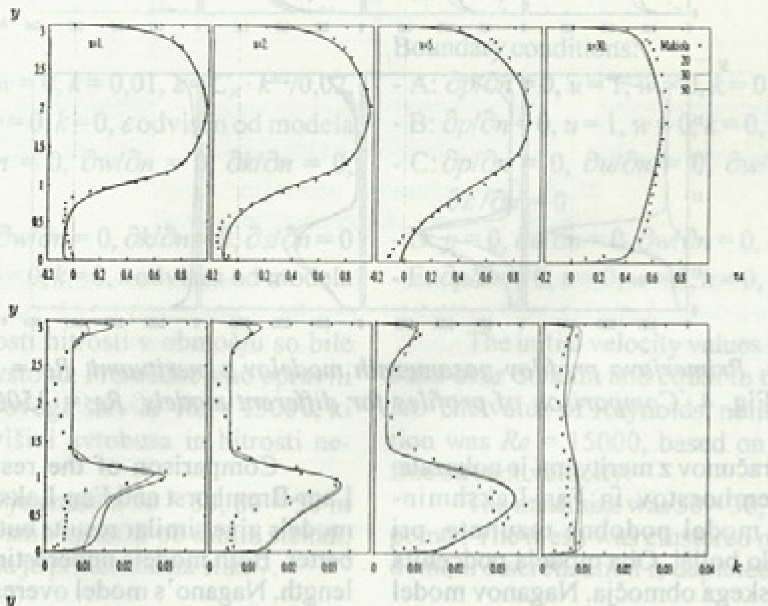

Sl. 3. *Primerjava profilov za različne gostote mrež, Re = 15000*
Fig. 3. *Comparison of profiles for different meshes, Re = 15000*

Profili hitrosti se z zgoščevanjem mreže bistveno ne spremenijo. Prav tako se veliko ne spremenijo profili turbulentne kinetične energije. Večje razlike so pri turbulentnem raztrosu. Sklepamo lahko, da smo dobili od mreže neodvisno rešitev.

Na sliki 4 je prikazana primerjava izračunanih profilov hitrosti, turbulentne kinetične energije in turbulentnega raztrosa z izmerjenimi vrednostmi. Primerjali smo profile vseh treh uporabljenih modelov na različnih oddaljenostih od stopnice (*X/S*=1, 2, 5 in 30).

Velocity profiles do not change much with mesh clustering. The same is valid for turbulent kinetic energy profiles. Slightly bigger differences are found in turbulent dissipation. We can presume that we have obtained a mesh independent solution.

In Figure 4 comparison is given of calculated velocity profiles, turbulent kinetic energy and turbulent dissipation profiles between three turbulence models. The profiles were taken on different distances from the inlet (*X/S*=1, 2, 5 in 30).

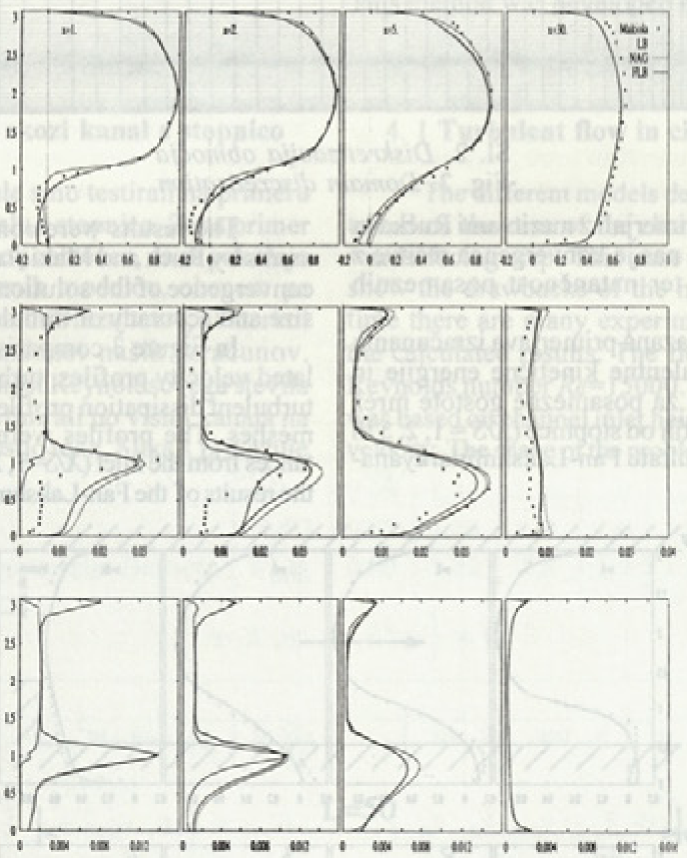

Sl. 4. *Primerjava profilov posameznih modelov z meritvami, Re = 15000*
Fig. 4. *Comparison of profiles for different models, Re = 15000*

Primerjava izračunov z meritvami je pokazala, da dajeta Lam-Bremhorstov in Fan-Lakshminarayana-Barnettov model podobne rezultate, pri čemer je slednji malo boljši. Oba modela podcenita dolžino recirkulacijskega območja. Naganov model recirkulacijsko dolžino preceni, izračunani profili hitrosti pa se precej bolje ujemajo z meritvami kakor pri prvih dveh modelih, vendar na račun daljšega časa izračuna.

Comparison of the results showed that the Lam-Bremhorst and Fan-Lakshminarayana-Barnett models give similar results but the second is slightly better. Both models underestimate the recirculation length. Nagano's model overestimates recirculation length, and the calculated profiles are in better agreement with the measurements than in both previous models, but the price for better results is longer computational time.

4.2 Turbulentni tok okoli vozila

Za praktični primer uporabe turbulentnih modelov z dušilnimi funkcijami smo preračunali tokovne razmere okoli obrisa avtobusa mestnega prometa. Avtobus je prikazan na sliki 5.

4.2 Turbulent flow past vehicle

To prove the practical meaning of turbulence low-Reynolds models we calculated the flow field around a city traffic bus. The bus is shown in Figure 5.

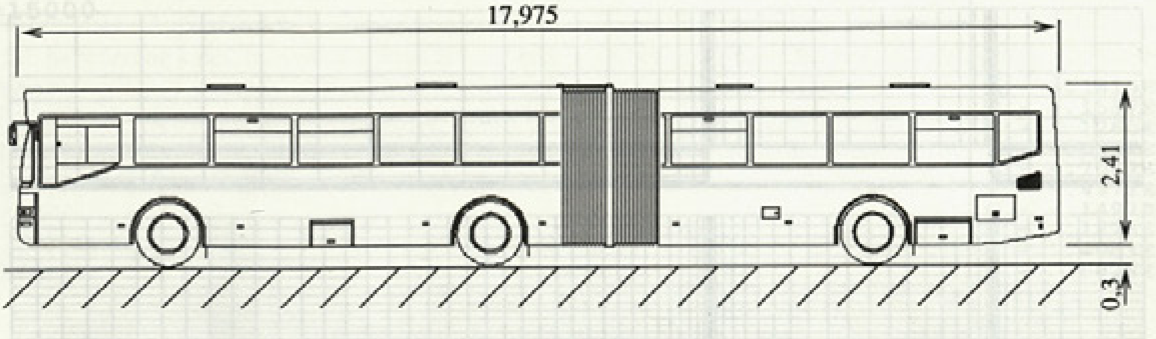

Sl. 5. *Avtobus: mere v metrih*
Fig. 5. *Bus: dimensions in metres*

Na sliki 6 je prikazan problem v brezdimenzijskih enotah. Kot referenčno dolžino smo uporabili višino avtobusa L = 2,41 m.

In Figure 6 the problem is depicted in nondimensional units. The height of the bus was used as the unit for nondimensionalization. The original height of the bus was L = 2.41 m.

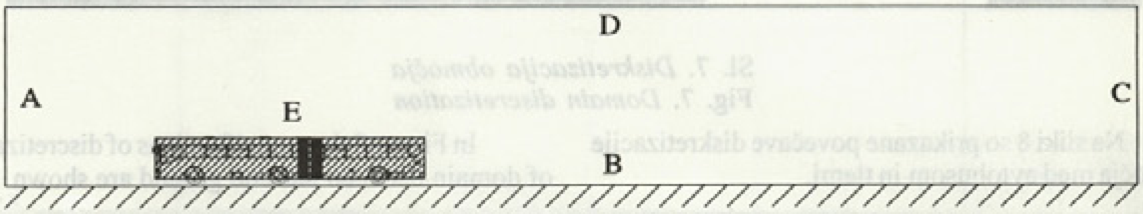

Sl. 6. *Avtobus: območje in robne razmere*
Fig. 6. *Bus: domain and boundary conditions*

Robne razmere:
- A: $\partial p/\partial n = 0$, $u = 1$, $w = 0$, $k = 0{,}01$, $\varepsilon = C_\mu \cdot k^{3/2}/0{,}02$,
- B: $\partial p/\partial n = 0$, $u = 1$, $w = 0$, $k = 0$, ε odvisen od modela
- C: $\partial p/\partial n = 0$, $\partial u/\partial n = 0$, $\partial w/\partial n = 0$, $\partial k/\partial n = 0$, $\partial \varepsilon/\partial n = 0$
- D: $p = 0$, $\partial u/\partial n = 0$, $\partial w/\partial n = 0$, $\partial k/\partial n = 0$, $\partial \varepsilon/\partial n = 0$
- E: $\partial p/\partial n = 0$, $u = 0$, $w = 0$, $k = 0$, ε odvisen od modela

Boundary conditions:
- A: $\partial p/\partial n = 0$, $u = 1$, $w = 0$, $k = 0.01$, $\varepsilon = C_\mu \cdot k^{3/2}/0.02$,
- B: $\partial p/\partial n = 0$, $u = 1$, $w = 0$, $k = 0$, ε depends on model
- C: $\partial p/\partial n = 0$, $\partial u/\partial n = 0$, $\partial w/\partial n = 0$, $\partial k/\partial n = 0$, $\partial \varepsilon/\partial n = 0$
- D: $p = 0$, $\partial u/\partial n = 0$, $\partial w/\partial n = 0$, $\partial k/\partial n = 0$, $\partial \varepsilon/\partial n = 0$
- E: $\partial p/\partial n = 0$, $u = 0$, $w = 0$, $k = 0$, ε depends on model

Začetne vrednosti hitrosti v območju so bile enake vrednostim na vstopu. Preračune smo opravili za vrednost Reynoldsovega števila Re = 15000, ki smo ga določili po višini avtobusa in hitrosti neoviranega pretoka.

Velikost mreže je znašala 50 × 30, 80 × 50 in 120 × 80 točk. Mrežo smo zgostili ob trdnih stenah. Diskretizacija območja je prikazana na sliki 7.

The initial velocity values in domain were constant over domain and equal to the values on the inlet. The value of Reynolds' number for the calculation was Re = 15000, based on the bus height and free stream velocity.

The mesh size was 50 × 30, 80 × 50 and 120 × 80 points. The mesh was clustered near solid walls. The domain discretization is depicted in Figure 7.

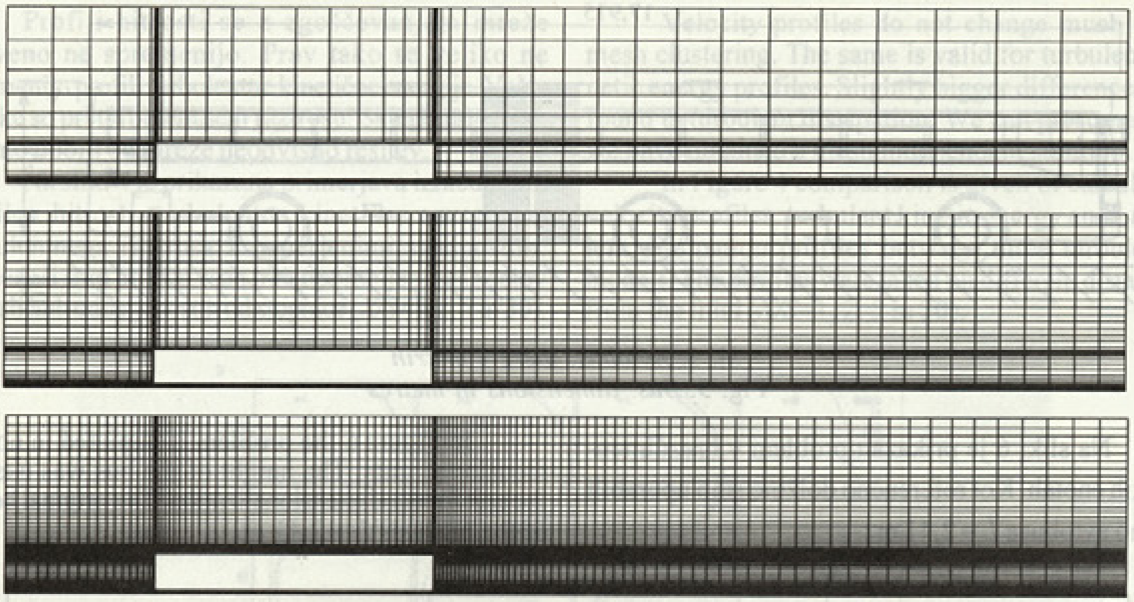

Sl. 7. *Diskretizacija območja*
Fig. 7. *Domain discretization*

Na sliki 8 so prikazane povečave diskretizacije področja med avtobusom in tlemi.

In Figure 8 the magnifications of discretization of domain between bus and ground are shown.

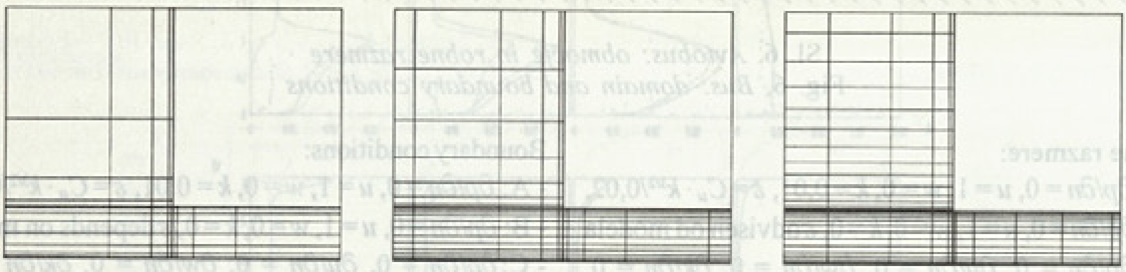

Sl. 8. *Diskretizacija območja: detajl*
Fig. 8. *Domain discretization: detail*

Rezultate izračunov smo primerjali z rezultati programa FIDAP, ki je izdelek podjetja Fluid Dynamics International. FIDAP temelji na metodi končnih elementov, za modeliranje turbulence pa uporablja običajni model k-ε z zidnimi funkcijami.

The results of calculation were compared with results of program FIDAP, that is a product of Fluid Dynamics International. FIDAP is based on the finite element method and uses standard k-ε model with wall functions for turbulence modeling.

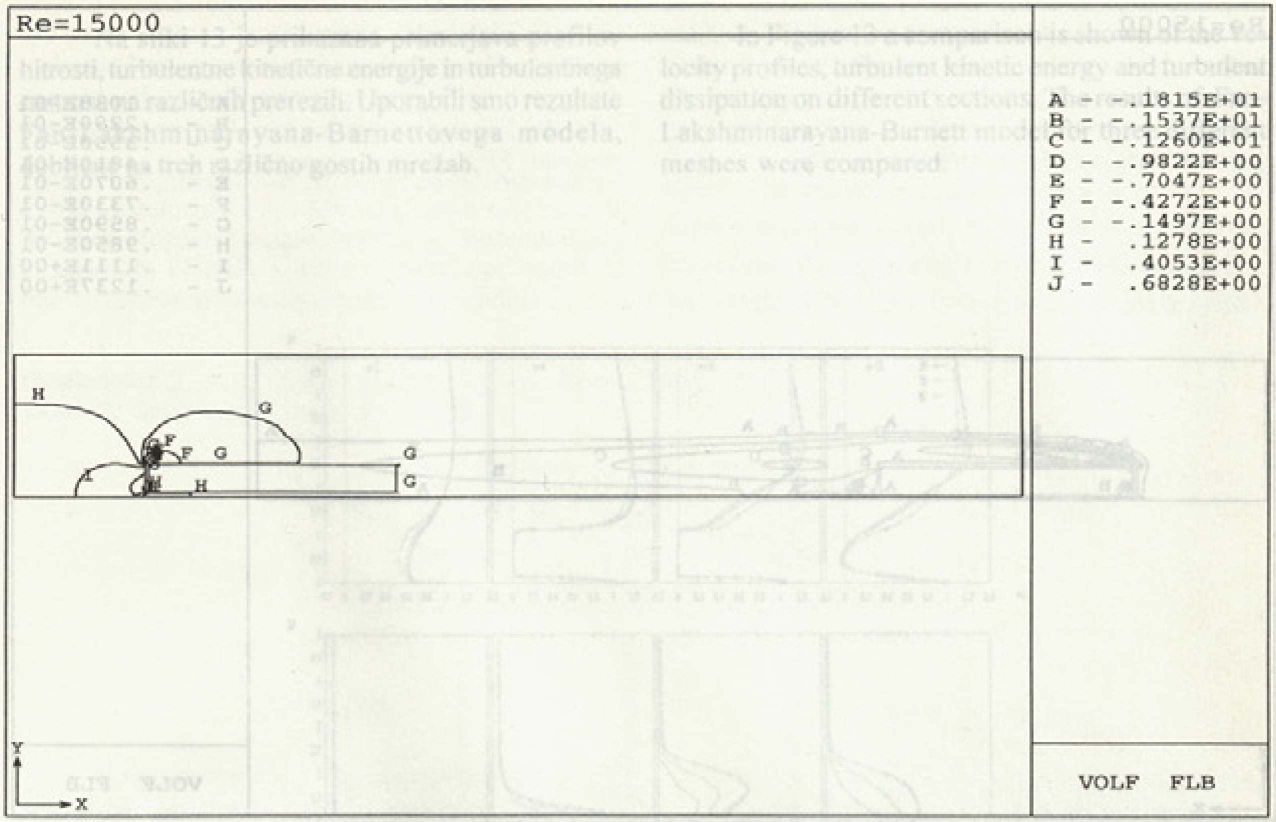

Sl. 9. *Tlačno polje, Re = 15000*
Sl. 9. *Pressure field, Re = 15000*

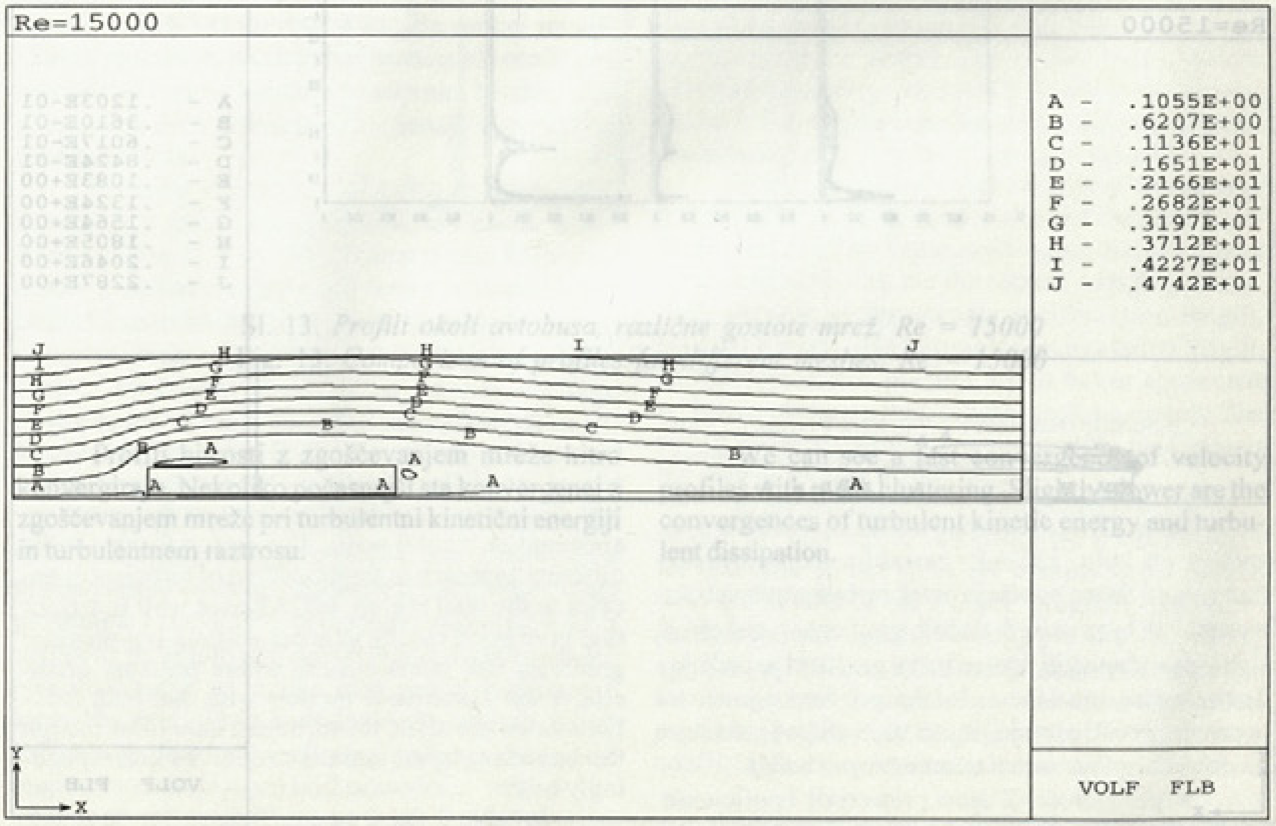

Sl. 10. *Tokovnice, Re = 15000*
Fig. 10. *Streamlines, Re = 15000*

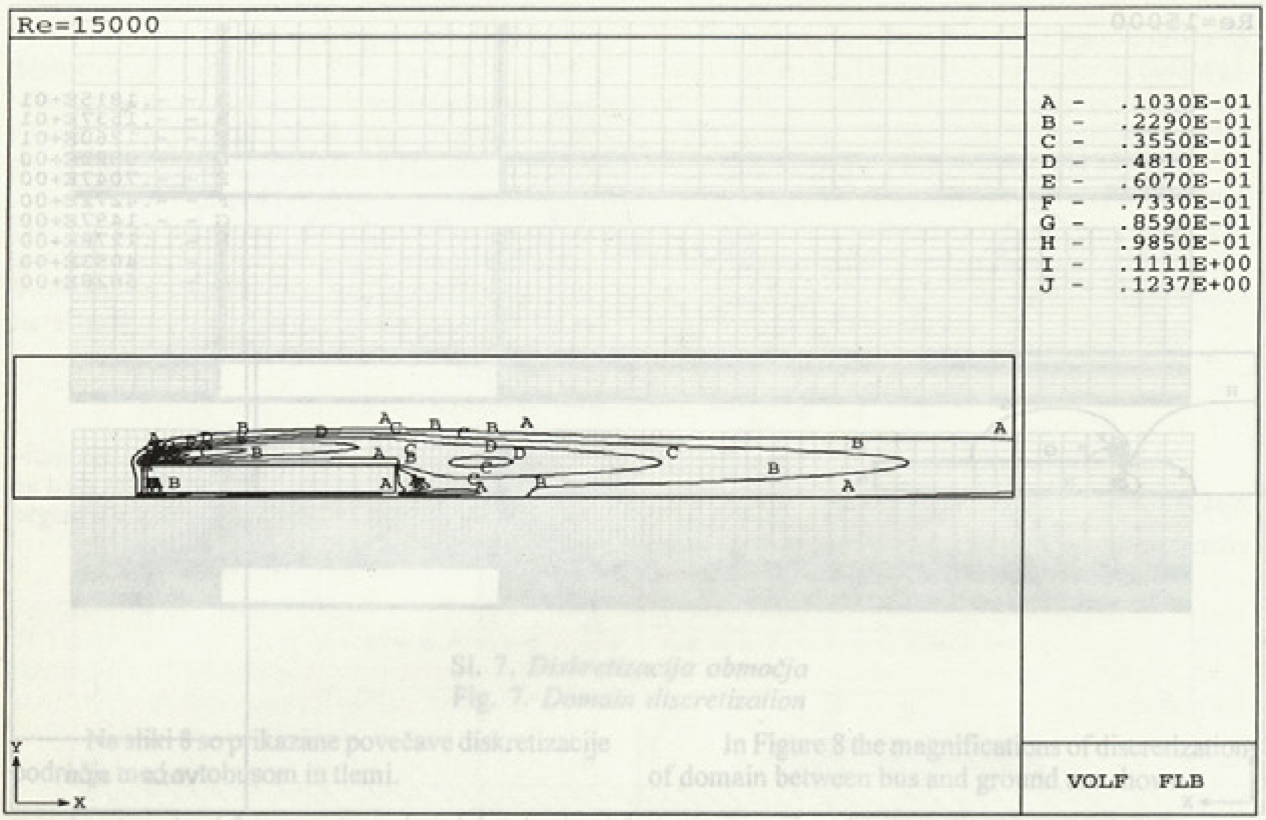

Sl. 11. *Turbulentna kinetična energija, Re = 15000*
Fig. 11. *Turbulent kinetic energy, Re = 15000*

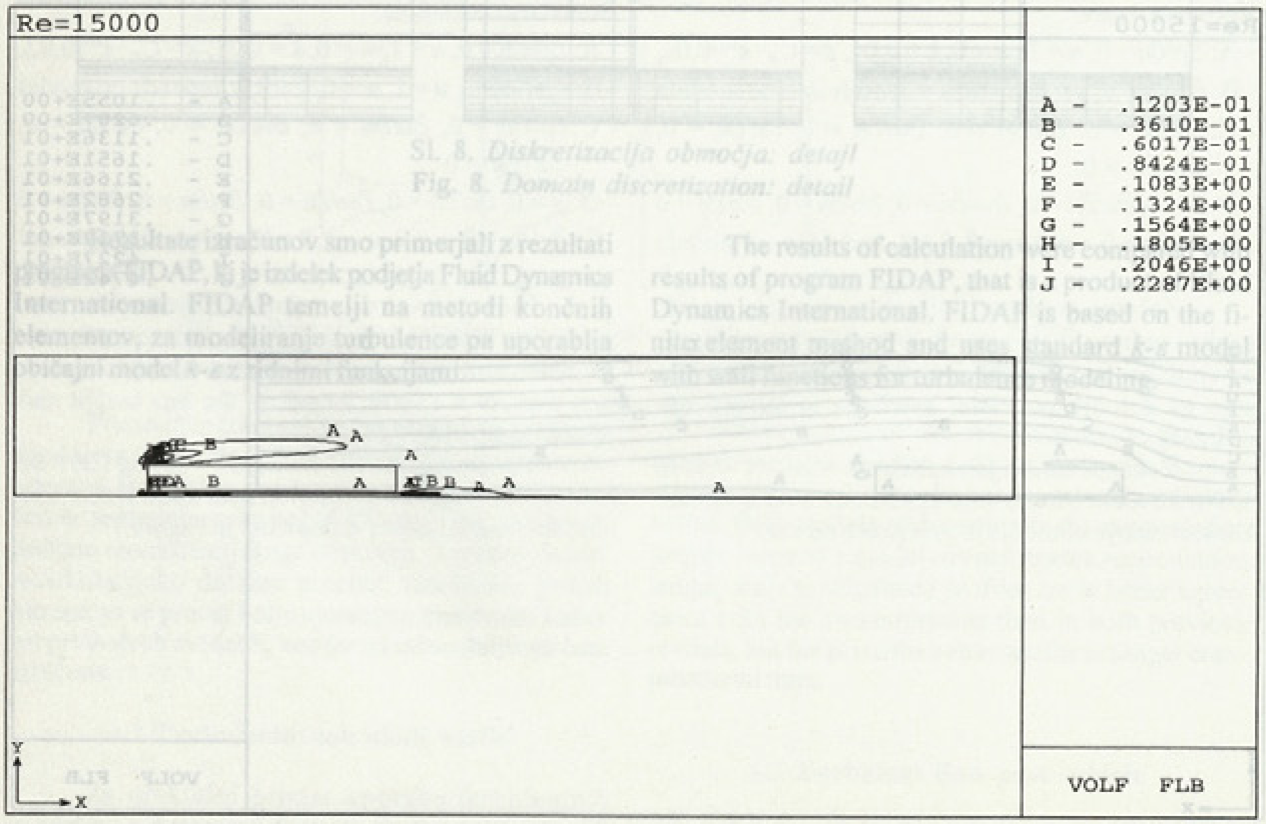

Sl. 12. *Turbulentni raztros, Re = 15000*
Fig. 12. *Turbulent dissipation, Re = 15000*

Na sliki 13 je prikazana primerjava profilov hitrosti, turbulentne kinetične energije in turbulentnega raztrosa na različnih prerezih. Uporabili smo rezultate Fan-Lakshminarayana-Barnettovega modela, dobljene na treh različno gostih mrežah.

In Figure 13 a comparison is shown of the velocity profiles, turbulent kinetic energy and turbulent dissipation on different sections. The results of Fan-Lakshminarayana-Barnett model for three different meshes were compared.

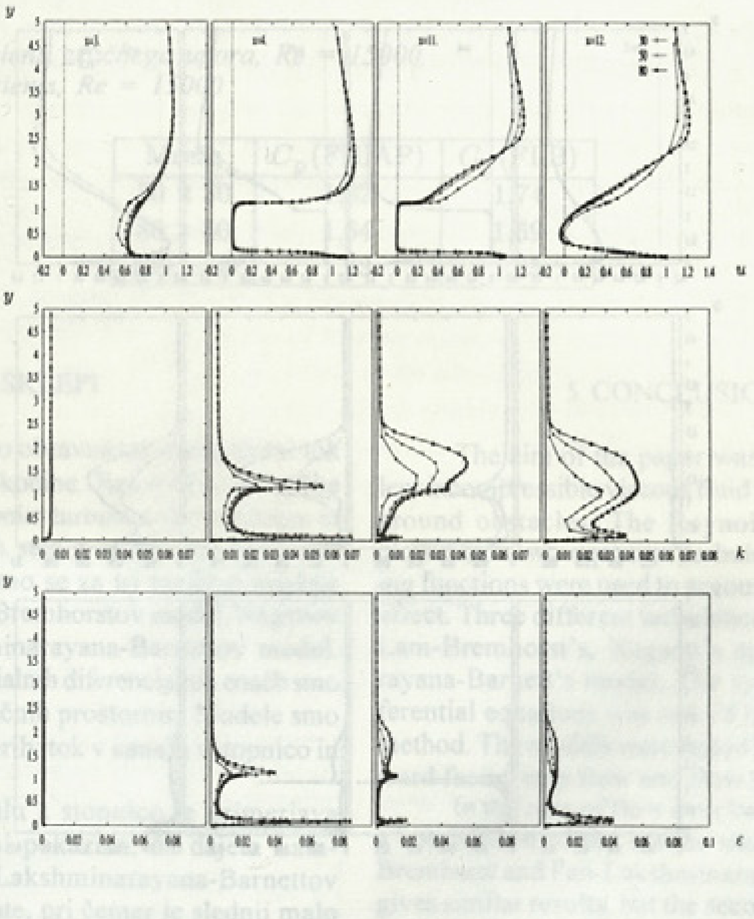

Sl. 13. *Profili okoli avtobusa, različne gostote mrež, Re = 15000*
Fig. 13. *Comparison of profiles for different meshes, Re = 15000*

Profili hitrosti z zgoščevanjem mreže hitro konvergirajo. Nekoliko počasnejši sta konvergenci z zgoščevanjem mreže pri turbulentni kinetični energiji in turbulentnem raztrosu.

We can see a fast convergence of velocity profiles with mesh clustering. Slightly slower are the convergences of turbulent kinetic energy and turbulent dissipation.

Na sliki 14 je prikazana primerjava profilov hitrosti, turbulentne kinetične energije in turbulentnega raztrosa v različnih prerezih. Primerjali smo rezultate, dobljene s programom FIDAP, ter rezultate Fan-Lakshminarayana-Barnettovega modela.

In Figure 14 a comparison is shown of the velocity profiles, turbulent kinetic energy and turbulent dissipation on different sections. The results obtained with the Fan-Lakshminarayana-Barnett model and program FIDAP were compared.

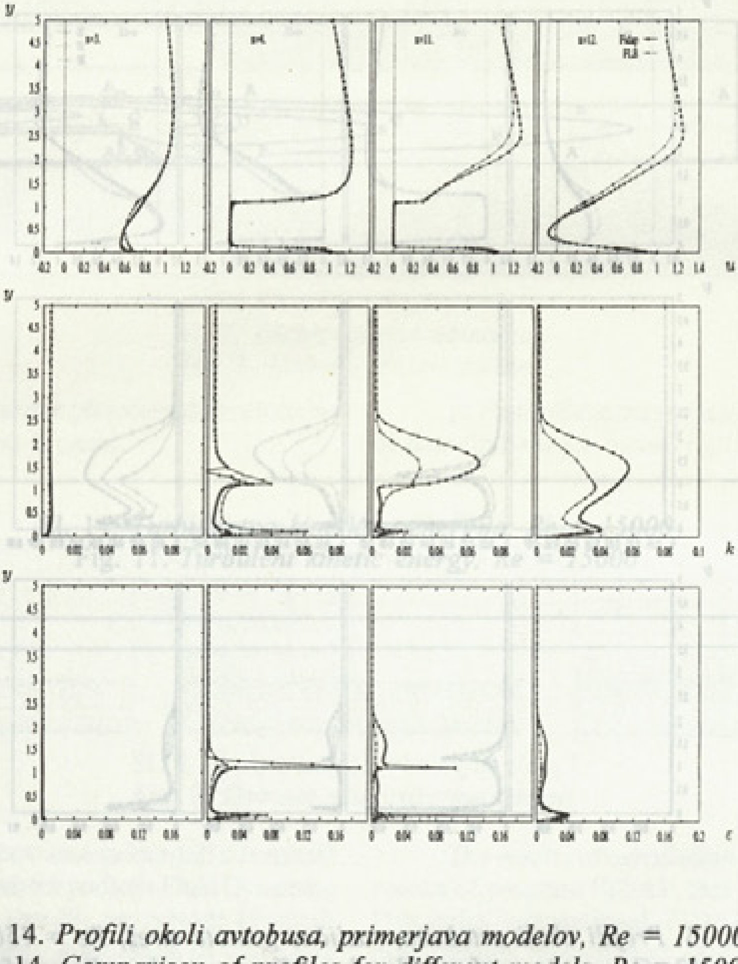

Sl. 14. *Profili okoli avtobusa, primerjava modelov, Re = 15000*
Fig. 14. *Comparison of profiles for different models, Re = 15000*

Ujemanje rezultatov programa FIDAP in Fan-Lakshminarayana-Barnettovega modela je ustrezno. Največje razlike se pojavijo ob trdnih stenah, kar je posledica različnega postopka modeliranj turbulentnih veličin ob zidu. FIDAP uporablja namreč zidne funkcije, ki dobro popišejo potek turbulentnih veličin v območjih brez velikih tlačnih gradientov, nekoliko slabše pa v območjih, kjer se tlačni gradienti pojavljajo. Turbulentni modeli z dušilnimi funkcijami te pomanjkljivosti nimajo, saj se vse veličine računajo tik do zidu in so rezultati temu ustrezno boljši.

V preglednici 2 smo primerjali koeficiente zračnega upora za vse tri mreže. Koeficiente zračnega upora smo računali z izrazom:

The comparison showed that the velocity profiles are in good agreement. Greater differences appeared in turbulent kinetic energy profiles and turbulent dissipation profiles. The greatest disagreement appeared near solid walls. The reason for that is the different approach to the modelling of turbulent quantities in the wall region. FIDAP uses wall functions that give good results in areas without big pressure gradients and worse results where pressure gradients arise. Turbulence models with dumping functions calculate all of the turbulent quantities though the boundary layer, and the results are correspondingly better.

In table 2 the drag coefficients for three different meshes are presented. Drag coefficients were calculated with the expression:

$$C_D = \frac{F_x}{\frac{1}{2}\rho v^2},$$

kjer je F_x rezultirajoča sila, ki deluje na avtobus v smeri x, ρ je gostota zraka in v hitrost gibanja avtobusa. V drugem stolpcu imamo rezultate, izračunane s programom FIDAP, v tretjem stolpcu pa rezultate Fan-Lakshminarayana-Barnettovega modela.

where F_x is resulting force on bus in x direction, ρ air density and v bus speed. In the second column are the results of program FIDAP, and the third column the results of Fan-Lakshminarayana-Barnett model.

Preglednica 2. *Koeficienti zračnega upora, Re = 15000*
Table 2. *Drag coefficients, Re = 15000*

Mreža	C_D(FIDAP)	C_D(FLB)
50 × 30	1,82	1,74
80 × 50	1,64	1,69
120 × 80	1,63	1,65

5 SKLEPI

V prispevku smo obravnavali turbulentni tok nestisljive viskozne tekočine. Reynoldsove enačbe smo sklenili z dvoenačbnim turbulentnim modelom in upoštevali vpliv trdnih sten z različnimi dušilnimi funkcijami. Odločili smo se za tri različne modele dušilnih funkcij: Lam-Bremhorstov model, Naganov model in Fan-Lakshminarayana-Barnettov model. Ohranitveni sistem parcialnih diferencialnih enačb smo reševali po metodi končnih prostornin. Modele smo preverili na dveh primerih: tok v kanalu s stopnico in tok okoli vozila.

Pri toku v kanalu s stopnico je primerjava izračunov z meritvami pokazala, da dajeta Lam-Bremhorstov in Fan-Lakshminarayana-Barnettov model podobne rezultate, pri čemer je slednji malo boljši. Oba modela podcenita dolžino recirkulacijskega območja. Naganov model recirkulacijsko dolžino preceni, izračunani profili hitrosti pa se precej bolje ujemajo z meritvami kakor pri prvih dveh modelih. Do razlike pride zaradi uporabe različnih parametrov v dušilnih funkcijah.

V drugem primeru smo računali tokovno polje okoli avtobusa mestnega prometa. Ker meritev tega primera nismo imeli, smo rezultate primerjali z rezultati programa FIDAP. Po primerjavi rezultatov smo ugotovili, da se hitrostni profili precej dobro ujemajo. Nekoliko večje so razlike med profili turbulentne kinetične energije in turbulentnega raztrosa.Kljub vsemu so razlike med koeficienti zračnega upora zelo majhne in znašajo manj ko 2 odstotka.

5 CONCLUSIONS

The aim of the paper was to study the turbulent incompressible viscous fluid flow in channels and around obstacles. The Reynolds equations were closed by a two-equation turbulence model. Dumping functions were used to account for the solid walls effect. Three different turbulence models were used: Lam-Bremhorst's, Nagano's and Fan-Lakshminarayana-Barnett's model. The system of partial differential equations was solved by the finite volume method. The models were tested for the case of backward facing step flow and flow past vehicle.

In the case of flow over backward facing step, a comparison of the results showed that the Lam-Bremhorst and Fan-Lakshminarayana-Barnett model gives similar results, but the second is slightly better. Both models underestimate recirculation length. Nagano's model overestimates recirculation length, and the calculated profiles are in better agreement with measurements than in both previous models. The use of different parameters in dumping functions is the reason for this difference.

In the second case we calculated the flow field around the city traffic bus. Since the measurements for that case do not exist, we compared our results with the results of the FIDAP program. The comparison showed that the velocity profiles are in good agreement. Greater differences appeared in turbulent kinetic energy profiles and turbulent dissipation profiles. Despite this the differences between drag coefficients are quite small, less than 2 percent.

6 LITERATURE
6 REFERENCES

[1] Fan, S., Lakshminarayana, B., Barnett, M.: A Low-Reynolds Number k-ε Model for Unsteady Turbulent Boundary Layer Flows. AIAA Journal, 1993.

[2] Drikakis, D., Govatsos, P.A., Papantonis, D.E.: A Characteristic-Based Method for Incompressible Flows. Int. J. Numer. Meth. Fluids, 19, 667-685, 1994.

[3] Lam, C.K.G., Bremhorst, K.A.: Modified Form of k-ε Model for Predicting Wall Turbulence, ASME, J. Fluids Engineering, 103, 456-460, 1981.

[4] Nagano, Y., Kim, C.: Two-Equation Model for Heat Transport in Wall Turbulent Shear Flows, J. Heat Transfer, 110, 1988.

[5] Ruck B., Makiola, B.: Flow Separation Over the Step With Inclined Walls. Elsevier, 1993.

[6] Žunič, Z.: Numerična obravnava problema aerodinamike vozil. Magistrsko delo, Fakulteta za strojništvo Maribor, 1997.

Naslov avtorjev: mag. Zoran Žunič, dipl. inž.
prof. dr. Leopold Škerget, dipl. inž.
Fakulteta za strojništvo
Univerze v Mariboru
Smetanova 17
2000 Maribor

Authors' Address: Mag. Zoran Žunič, Dipl. Ing.
Prof. Dr. Leopold Škerget, Dipl. Ing.
Faculty of Mechanical Engineering
University of Maribor
Smetanova 17
2000 Maribor, Slovenia

Prejeto:
Received: 30.5.1997

Sprejeto:
Accepted: 15.12.1997